JOURNAL OF CATALYSIS 35, 206–217 (1974)

Concentration Profiles in Impregnation of Porous Catalysts*

RICHARD C. VINCENT AND ROBERT P. MERRILL

Department of Chemical Engineering, University of California, Berkeley, California 94720

Received February 21, 1974; revised May 31, 1974

Regulation of the depth and uniformity of the impregnation of catalyst support pellets with an active ingredient is of considerable industrial importance. A model for the time-dependent flow of impregnating solution into a dry pellet and interior dispersal of impregnant is presented. It consists of plug flow into a single pore with either mass transfer across the liquid–solid interface or adsorption kinetics providing resistance to the removal of impregnant from solution. Predictions based on the model are consistent with laboratory impregnations. Of three independent parameters, the relative capacity for adsorption is both the most important in regulating dispersal and the easiest to adjust in practice.

NOMENCLATURE

c	Concentration, moles/cm^3
c_s	Adsorption capacity per unit area of pore wall, moles/cm^2
c_0	Initial concentration
D	Dispersion coefficient, cm^2/sec
$\mathfrak{D}$	Diffusivity, cm^2/sec
k_m	Mass transfer coefficient, cm/sec
k_1	Adsorption rate coefficient, cm/sec
k_2	Desorption rate coefficient, moles/cm^2 sec
I	Impregnation of pore wall, moles/cm
K	Reduced mass transfer coefficient [Eq. (16)]
K_1	Reduced adsorption coefficient [Eq. (16)]
K_2	Reduced adsorption coefficient [Eq. (16)]
K_L	Langmuir equilibrium parameter, dimensionless
$l(t)$	Instantaneous penetration of liquid in pore, cm
L	Pore length, cm
r	Radial position, cm
R	Pore radius, cm
t	Time, sec
t_L	Time to fill pore completely with liquid, sec [Eq. (9)]
u	Reduced velocity [Eq. (4)]
$\mathbf{v}$	Vector velocity, cm/sec
v_p	Plug flow velocity, cm/sec
V	Rate of impregnant removal, moles/cm^3/sec
Z	Axial position, cm
α	Reduced diffusivity [Eq. (3)]
Γ	Reduced axial position [Eq. (3)]
λ	Surface tension, dyn/cm^2
μ	Solution viscosity, P
τ	Reduced time [Eq. (3)]
ψ	Reduced concentration [Eq. (3)]
ΔP	Pressure drop, dyn/cm^3
θ	Fractional coverage of adsorption sites

* Work Supported by NASA Grant No. NGR-05-003-478, Ames Research Laboratory, Moffit Field, CA.

INTRODUCTION

Many catalysts in common use consist of small metal crystallites dispersed on a high surface area support. Typically these dispersions are produced by impregnating a pellet or granule of the porous support with a liquid in which the catalytic ingredient is dissolved. During the impregnation and subsequent drying period, small crystallites of the catalyst or a compound containing the catalyst are de-

posited on the internal surface of the support material. Calcination and reduction, or other appropriate pretreatment techniques, may be necessary later on to convert the impregnant crystallite into a catalytically active form. Any of these steps can effect the particle size and final surface concentration of the catalytic material. In this paper the impregnation step is examined in order to find ways to predict and control radial profiles of the concentration of the active catalytic ingredient within the pellet.

The optimum composition profile may depend upon any of a variety of service conditions. If, for example, the reaction is severely mass-transfer limited, then the active material, usually a metal, should be deposited as close as possible to the external surface of the pellet or granule. The maximum metal dispersion and resistance to sintering normally occurs at the minimum surface concentration for a given metal loading (*1*, *2*). Therefore if mass transfer of reactants and products is rapid, optimum catalyst performance can be achieved by uniform impregnation.

In some situations it is even advantageous to produce a subsurface impregnation in which a band of catalyst-free support is established on the exterior of the pellet. If the reaction is poisoned by an impurity which is strongly adsorbed on the catalyst support, then the catalyst-free surface band can immobilize the poison, keeping it spatially separated from the active catalyst. Such a "chromatographic" separation of poison and catalyst can be used to extend the catalyst life and perhaps to ease the removal of the poison in subsequent regeneration steps. The subsurface impregnation can also be beneficial in service which produces catalyst attrition and loss of catalyst fines from the reactor space. A catalyst with a subsurface impregnation will attrit only the support and retain the active metal.

From these examples it is evident that prediction and control of the radial distribution of catalyst within a granule of support can often be employed to optimize catalyst performance. Though much is known empirically about producing desired composition profiles, the procedures used are often proprietary and there exists in the open literature little analytical or mechanistic information describing the important processes occurring during impregnation.

Maatman (*3*) has demonstrated that when alumina is impregnated with chloroplatinic acid, though there is a strong tendency toward surface impregnation, uniform impregnation can be obtained by adding HCl, HNO_3 or various inorganic nitrates to the impregnating solution. Apparently the additives compete with the chloroplatinic acid for available adsorption sites and cause surface saturation at much lower platinum levels, allowing the metal to penetrate deeper into the interior of the pellet.

Benesi, Curtis and Studer (*1*) have studied pH controlled ion exchange of metal cations with H^+ from alumina and silica supports. By absorbing the impregnating solution at sufficiently low pH, few adsorption sites (vacant basic sites) are available and the metal cations penetrate to the center of the solid. The H^+ in acidic solution which suppresses ion exchange can be regarded as an "additive" competing with the metal ions for potential adsorption sites.

Weisz (*4*) has examined in some detail the diffusional relaxation of concentration gradients along the length of catalyst pores and equilibration with bulk concentrations exterior to the pellet. The time constant for this relaxation, however, is generally long compared to impregnation times, so that employing this method to produce uniform impregnations would severely increase catalyst production times and they seldom will play a role in disturbing the profiles produced during impregnations when the drying process is carried out shortly after impregnation.

Methods

Modeling

The purpose of this work is to develop a tractable model for the transport and

deposition of material during the impregnation of a porous solid.

The problem is analogous to frontal chromatography on a scale small compared to the radius of the catalyst pellet. This situation is more complex than the simple chromatographic problem because the fluid flow into a catalyst pore never reaches a steady state. The overall pressure drop remains essentially constant and thus the pressure gradient decreases with time as the pore fills with liquid.

Appropriate modeling must be done in three areas:

1. Physical modeling of the porous solid.
2. Describing the controlling process for impregnant removal at the liquid–solid interface.
3. Hydrodynamic modeling for penetration of the liquid into the solid.

Models of porous solids are numerous, but the solution of the unsteady-state mass transport in a fluid flowing through tortuous channels characteristic of the actual pellet geometries would be a difficult task. Thus the idealized model of a single cylindrical pore will be analyzed in order to determine qualitatively the behavior of the type of system in question and identify the important parameters which will control impregnant concentration profiles. The results are compared, at least qualitatively, with laboratory observations of impregnation of three-dimensional alumina granules produced by ball-milling an alumina powder. In the single cylindrical pore solution begins to flow at time $t = 0$ (see Fig. 1) and penetrates deeply under capillary force, while impregnant molecules diffuse toward the wall and are removed from solution by adsorption. The capillary uptake is described by a model proposed by Washburn (*5*) which envisions the unsteady-state flow as a succession of Poiseuille steady states. It predicts a penetration rate proportional to $t^{-1/2}$. This model assumes a constant pressure drop (due to surface tension) in the pore, which applies strictly only if the pore were initially evacuated. If air in the pore has a channel of easy escape, however, then the constant pressure

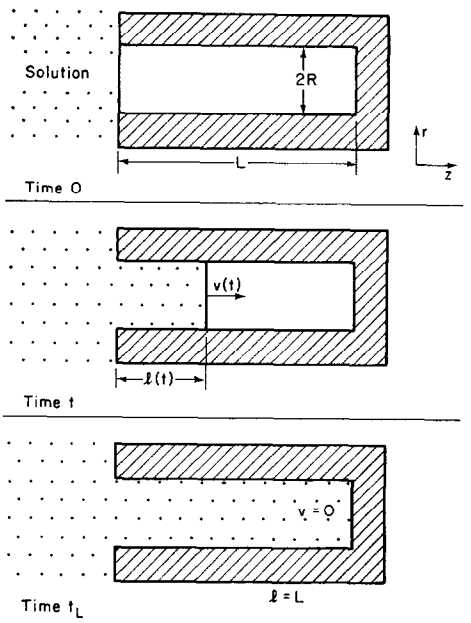

FIG. 1. Single pore model.

difference is certainly maintained. Since most porous pellets exude air during liquid uptake, this simplification seems amply justified. The rigorous mass balance, for sufficiently low concentrations of impregnating species, is given by

$$\frac{\partial c}{\partial t} + \mathbf{v}(r, z, t) \cdot \nabla c = \mathfrak{D}\left[\frac{1}{r}\frac{\partial}{\partial r} r \frac{\partial c}{\partial r} + \frac{\partial^2 c}{\partial z^2}\right]; \quad c = c(r, z, t), \quad (1)$$

with side conditions

$$c(r, 0, t) = c_0 \frac{\partial^2 c}{\partial z^2}\bigg|_{z=l(t)} = 0 \frac{\partial c}{\partial r}\bigg|_{r=0} = 0, \quad (1a)$$

indicating constant impregnant concentration at the pore mouth, no transport beyond the instantaneous liquid front, and radial symmetry. The boundary condition at $r = R$ will depend on the particular description of the adsorption rate at the wall. Note that at $t = 0$, the field of the equation vanishes ($l = 0$) and hence the initial condition is $c(r, 0, 0) = c_0$.

Plug Flow Velocity

Equation (1) would require the time-dependent velocity field $\mathbf{v}(r, z, t)$. Unsteady laminar flow into an empty tube is appar-

ently an unsolved problem. It is quite difficult for three reasons: (1) the flow is time-dependent, (2) the pressure gradient depends on the depth of penetration and (3) the radial component clearly approaches zero well back of the front of the liquid but is significant near the front if the usual condition of zero slip at $r = R$ is applied.

Instead of using the real (but unknown) $\mathbf{v}(r, z, t)$, one-dimensional plug flow $\mathbf{v}_p(t)$ was assumed. Such a substitution into Eq. (1) is valid *only* if there are no significant *radial concentration gradients*, since the existence of such gradients would introduce serious errors in the axial convection term $\mathbf{v}_p(\partial c/\partial z)$. On the other hand, if $\partial c/\partial r$ is negligible, the first term on the right of (1) is unimportant and the r dependence of (1) is completely removed.

The relative magnitude of $\partial c/\partial r$ can be estimated by calculating the dispersion coefficient D, where D has a value such that the solution to

$$\frac{\partial c}{\partial t} + v_p \frac{\partial c}{\partial z} = D \frac{\partial^2 c}{\partial z^2} \qquad (2)$$

will yield the same value of $c(z)$ as the mixing-cup average value of $c(r, z)$ from (1). D is given analytically (*6*, *7*) by $D = v_p^2 R^2/48\mathfrak{D}$ for laminar flow in long pipes when $(\partial c/\partial r)|_{r=R} = 0$. Using an average velocity $\langle v_p \rangle = L/t_L$, $L = 1$ cm, $t_L = 1$ sec, $R = 10^{-4}$ cm, $\mathfrak{D} = 10^{-5}$ cm^2/sec, there results $D = 2 \times 10^{-5}$ cm^2/sec. Thus, the characteristic time for axial dispersion along a length of pore of the order of the pore radius is comparable to radial diffusion times. Hence, for pores with $L/R \gg 1$, there is virtually no axial dispersion because of the radially dependent velocity profile and therefore essentially *no radial concentration gradients* for sufficiently concentrated solutions. The effect of concentration gradients very near the wall are discussed below in connection with removal mechanisms.

Equation (1), then, can be replaced by

$$\frac{\partial c}{\partial t} + v_p \frac{\partial c}{\partial z} = D \frac{\partial^2 c}{\partial z^2} + V(c, \theta), \qquad (3)$$

where V is some function describing the rate of removal of impregnant from the system. Defining $\Gamma = z/L$, $\psi = c/c_0$, $\tau = t/t_L$, $\alpha = Dt_L/L^2$ and $u = v_p t_L/L$, gives:

$$\frac{\partial \psi}{\partial \tau} + u \frac{\partial \psi}{\partial \Gamma} = \alpha \frac{\partial^2 \psi}{\partial \Gamma^2} + \frac{t_L}{c_0} V(c_0\psi, \theta). \qquad (4)$$

In practical situations, $\alpha < 10^{-4}$ and $(t_L/c_0)V \approx K\psi$ where $K \sim 1$, and the first term on the right of Eq. (4) is thus negligible. Finally, the approximate mass balance to be solved is

$$\frac{\partial \psi}{\partial \tau} + u \frac{\partial \psi}{\partial \Gamma} = \frac{t_L}{c_0} V(c_0\psi, \theta), \qquad (5)$$

$$\psi(0, \tau) = 1, \qquad \psi(0, 0) = 1.$$

Penetration rate: $v_p = dl/dt$

Washburn (*5*) has presented an empirically tested expression for the rate of penetration (identical to velocity for an incompressible liquid) into a capillary tube. If it is assumed that the time-dependent flow of the liquid column is a passage through an infinite succession of Poiseuille steady states, and the small inertial effects are neglected, the radial average velocity when the liquid front has reached a distance l into the capillary is:

$$\langle v \rangle(t) = dl/dt = \frac{R^2 \Delta P}{8 \mu l(t)}, \qquad (6)$$

Integrating,

$$l(t) = \frac{R}{2}\left(\frac{\Delta P}{\mu}\right)^{1/2} t^{1/2}, \qquad (7)$$

$$v_p = \langle v \rangle = \frac{R}{4}\left(\frac{\Delta P}{\mu}\right)^{1/2} t^{-1/2}. \qquad (8)$$

The time t_l required to penetrate a distance l is

$$t_l = \frac{4 l^2 \mu}{R^2 \Delta P}. \qquad (9)$$

In this work, ΔP was taken to be $\gamma/2R$ where γ is the surface tension of water, 72 dyn/cm^2 at 25°C.

Substituting (8), (9) and $u = v_p t_L/L$ into (5),

$$\frac{\partial \psi}{\partial \tau} + \frac{1}{2\tau^{1/2}} \frac{\partial \psi}{\partial \Gamma} = \frac{t_L}{c_0} V(c_0\psi, \theta). \qquad (10)$$

Model of Impregnant Removal at the Pore Wall

Simplifying the mass balance so as to remove the radial coordinate is mathematically equivalent to assuming that there is no resistance in the liquid to radial transport of impregnant. In the absence of some kind of resistance to removal of impregnant at or near the pore wall, V would necessarily be very large compared to c_0/t_L. This would result in the unintercesting cases in which the pore mouth would adsorb all the impregnant or, if there is a saturation limit, the pore wall would be saturated ($\theta = 1$) near the mouth with an abrupt change to $\theta = 0$ at some value of Γ depending on the adsorption capacity of the pore wall. This latter case was verified by solving the mass balance equations for diffusional resistance to radial transport in the bulk liquid under real plug flow with instantaneous removal at the wall:

$$\frac{\partial c}{\partial t} + v_p \frac{\partial c}{\partial z} = \mathfrak{D} \frac{1}{r} \frac{\partial}{\partial r}\left(\frac{1}{r}\frac{\partial c}{\partial r}\right), \qquad (11)$$

$$\frac{\partial \theta}{\partial t} = \frac{\mathfrak{D}}{c_0 R} \frac{\partial c}{\partial r}\bigg|_{r=R},$$

$$c(z, r, t) = 0 \text{ for } \theta < 1,$$

$$\frac{\partial c}{\partial r}\bigg|_{r=R} = 0 \text{ for } \theta = 1, \frac{\partial c}{\partial r}\bigg|_{r=0} = 0.$$

Note that the rate of adsorption changes from instantaneous to zero when $\theta = 1$. As the reduced diffusivity $\mathfrak{D}t_L/R^2$ was increased to realistic (large) values, the coverage θ became a step-function in Γ, as expected (see Appendix for a description of the solution method).

That such a step-function of θ vs Γ does not always occur in real systems is suggested by the electron microprobe studies of Andersen and Chen (*8*) which show gradual impregnant profiles of metal in alumina pellets. Thus, in Eq. (5) the removal function $V(C, \theta)$ should include a finite resistance for the deposition process. Two such resistances often considered were investigated: mass transfer resistance in the liquid at the phase boundary and the adsorption kinetics. Both are consistent with the assumption of no radial concentration gradients in the bulk liquid. When the resistance is due to adsorption kinetics, the concentration is uniform over the entire pore radius. In the mass transfer limiting case, the model consists of uniform concentration in the bulk liquid with a concentration gradient confined to a thin layer adjacent to the wall providing the driving force to mass transfer (film model).

Impregnant Removal at Pore Wall

1. Control by mass transfer. A conventional mass transfer coefficient is used:

$$V = \frac{-2k_m}{R}(c - c_w),$$

where k_m has units cm sec^{-1}, $2/R$ is the surface area to volume ratio of the pore and c_w is the concentration adjacent to the wall. c_w is assumed to be in equilibrium with the adsorbed phase characterized by the Langmuir isotherm

$$\theta = \frac{K'_L c_w}{1 + K'_L c_w}. \qquad (12)$$

The surface fractional coverage θ is determined by

$$\frac{\partial(\theta c_S)}{\partial t} = k_m(c - c_w). \qquad (13)$$

Applying (11) and nondimensionalizing, the equations for this case result in:

$$\frac{\partial \psi}{\partial \tau} + \frac{1}{2\tau^{1/2}} \frac{\partial \psi}{\partial \Gamma} = -K\left(\psi - \frac{\theta}{K_L(1-\theta)}\right), \qquad (14a)$$

$$\frac{\partial \theta}{\partial \tau} = \frac{K}{\eta}\left(\psi - \frac{\theta}{K_L(1-\theta)}\right), \qquad (14b)$$

where

$$K = \frac{2k_m t_L}{R}, \qquad \eta = \frac{2c_S}{Rc_0}, \qquad K_L = K'_L c_0.$$

Thus three independent variables describe the impregnation K, a reduced mass transfer coefficient; η, a relative capacity of the pore wall for adsorption, and K_L, an equilibrium adsorption coefficient.

2. Control by adsorption kinetics. In this case, the removal of impregnant at the wall is described by a reversible solute–solid reaction:

$$V = \frac{-2k_1}{R} c(1 - \theta) + \frac{2k_2}{R} \theta, \quad (15a)$$

$$\frac{\partial(\theta c_S)}{\partial t} = k_1 c(1 - \theta) - k_2 \theta. \quad (15b)$$

Equations (10) and (14b) become

$$\frac{\partial \psi}{\partial \tau} + \frac{1}{2\tau^{1/2}} \frac{\partial \psi}{\partial \Gamma} = -K_1 \psi(1 - \theta) + K_2 \theta, \quad (16a)$$

$$\frac{\partial \theta}{\partial \tau} = \frac{K_1}{\eta} \psi(1 - \theta) - \frac{K_2}{\eta} \theta, \quad (16b)$$

where

$$K_1 = \frac{2k_1 t_L}{R}, \quad K_2 = \frac{2k_2 t_L}{R c_0}, \quad \eta = \frac{2c_S}{R c_0}.$$

For $\partial\theta/\partial\tau = 0$, we have $\theta = (K_1/K_2\psi)/[1 + (K_1/K_2\psi)]$ or $\theta = K'_L\psi/(1 + K_L\psi)$ if $K_L = k_1/k_2$ so that an exact parallel exists between this and the former case. The only differences is the functional dependence of θ and the reduced reaction rate constant K_1 compared to the reduced mass transfer coefficient K (see Table 1). Of the three parameters, η is clearly the most easily controlled in practice (by controlling c_0).

2a. Irreversible adsorption kinetics. An interesting limiting case of the kinetically controlled model is one in which $K_L = \infty$ and θ is removed from the equations (i.e., there is no saturation limit). Such a model may apply if the adsorption process is actually crystallite growth or if a saturation limit does exist but is never approached because c_0 is small. As discussed below, this model may apply to ion-exchange impregnation.

Equation (10) becomes

$$\frac{\partial \psi}{\partial \tau} + \frac{1}{2\tau^{1/2}} \frac{\partial \psi}{\partial \Gamma} = -K\psi, \quad \psi(0, \tau) = 1. \quad (17)$$

Equation (17) has an analytical solution given by

$$\Psi = \exp(K\Gamma^2 - 2K\Gamma\tau^{1/2}). \quad (18)$$

The total impregnation, I, a distance Γ down the pore is given by

$$I(\Gamma) = c_0 \frac{R}{2} \int_{\tau=\Gamma^2}^{\tau=1} K\Psi d\tau, \quad (19)$$

TABLE 1

Limiting process:	Mass transfer		Kinetics
Parameters	K	$\leftrightarrow$	K_1
	K_L	$\leftrightarrow$	K_1/K_2
	η	$\leftrightarrow$	η

or

$$\frac{I}{c_0 R} = \left(\frac{1}{2} + \frac{1}{4K\Gamma^2}\right) \exp(-K\Gamma^2) - \left(\frac{1}{2\Gamma} + \frac{1}{4K\Gamma}\right) \exp(K\Gamma^2 - 2K\Gamma). \quad (20)$$

Results and Interpretation

Equations (15) and (16) were solved numerically, using a first-order finite difference technique. Values for the fractional coverage, θ, were computed for two situations: (1) at $\tau = 1$, i.e., as the pore just fills entirely with liquid and (2) at $\tau = \infty$, assuming that all impregnant still in solution ultimately adsorbs and/or crystallizes without further axial transport. The results for $\tau = 1$ are plotted in Figs. 2 and 3 as θ vs Γ and are compared in Fig. 4 with results for $\tau = \infty$.

Before considering the shapes of the plots, it is evident that the mass transfer and kinetic models give very nearly the same results, suggesting that within the framework of the entire model, it is unimportant how the removal at the wall is described. Henceforth, the independent parameters are referred to as K, K_L and η without regard to a particular description of the removal process. The parameters represent, respectively, an intrinsic rate of removal from the liquid, a measure of adsorption equilibrium and relative capacity for adsorption.

Figure 3 shows the results for a large value of K (low resistance to removal), $K = 10$. The curves are sigmoid generally, with the location of the "break" determined by η. The larger the capacity for adsorption, the nearer to the pore mouth the break occurs. K_L determines the steepness of the sigmoidal curve. The impregnant is more dispersed as the adsorption becomes more reversible. However, for low values

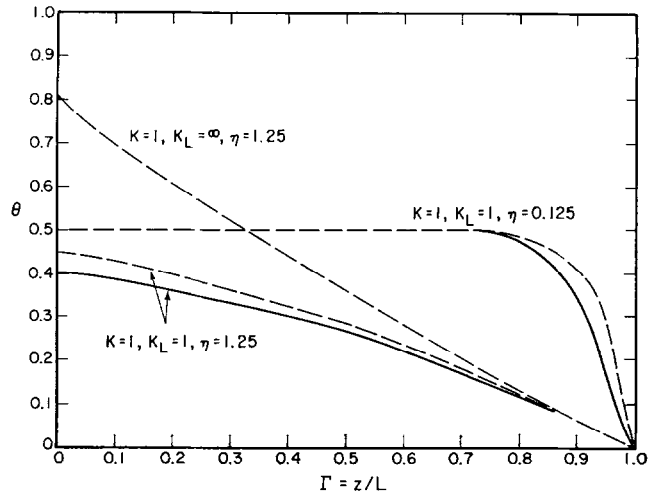

FIG. 2. Fractional coverage of pore wall vs axial position for a slowly adsorbing impregnant ($K = 1$) at $\tau = 1$. (—) Kinetic control; (- -) mass transfer control.

of η (nearly completely saturated pore) this effect of K_L on the breakthrough disappears.

The curves in Fig. 2 are for $K = 1$ (high resistance to removal). For high values of η, θ falls smoothly down the pore because the impregnant is dispersed axially before it is removed from solution. K_L becomes an unimportant parameter. For small η, the curves again become sigmoidal with a well-defined breakthrough.

The effects of the three parameters are strongly interconnected, evidently, over certain ranges. The conclusions which can be reasonably drawn from Figs. 2 and 3 are:

1. For sufficiently large η, the removal parameter K controls dispersion of impregnant. Low values of K give a smoothly decreasing concentration down the pore; high values given a sigmoidal profile.

2. For large K and η, the equilibrium parameter K_L, affects the slope of the pro-

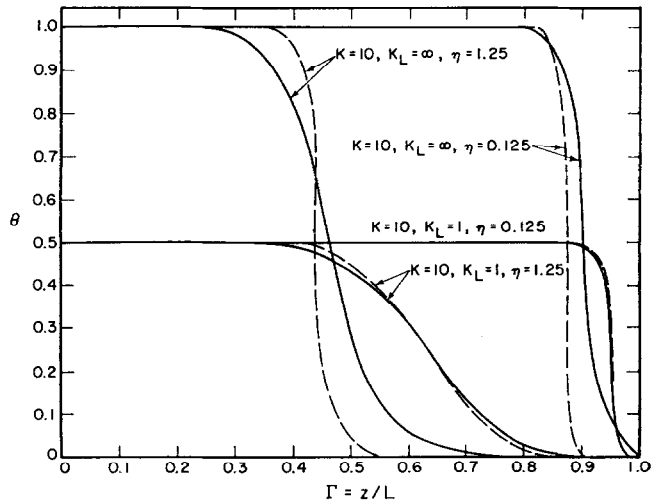

FIG. 3. Fractional coverage of pore wall vs axial position for a quickly adsorbing impregnant ($K = 10$) at $\tau = 1$. (—) Kinetic control; (- -) mass transfer control.

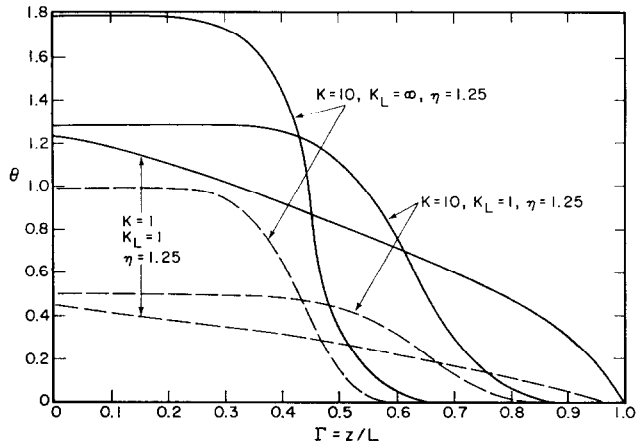

FIG. 4. Fractional coverage of pore wall vs axial position compared between $\tau = 1$ and $\tau = \infty$. (—) $\tau = \infty$; (- -) $\tau = 1$.

file at breakthrough. K_L has little effect if K is small.

3. For values of K large enough to saturate part of the pore, η controls the length of the saturated portion.

Finally, it is apparent from Fig. 4 that the three conclusions above are not affected qualitatively by the ultimate adsorption of whatever impregnant remains in solution when the pore fills with liquid. The difference in θ vs Γ between $\tau = 1$ and $\tau = \infty$ is approximately one of expanding the scale of θ by a constant factor.

The assumption behind the $\tau = \infty$ case shown in Fig. 4 is that the time for removal of the excess impregnant at $\tau = 1$ is much less than the time for axial diffusion down the pore. The case of axially mobile impregnant through a stagnant fluid filling the pore is treated thoroughly by Weisz (*4*).

Figure 5 shows the solution to Eq. (20) (the case for nonsaturation of the pore wall) for several values of K. Small values of K result in uniform adsorption, but the concentration level cannot easily be controlled.

Relation of the Model to Real System

If a real porous body is envisioned as a tortuous collection of interconnected pores all of which have a very large length to diameter ratio, the results of the single pore model described here should be extendable to a real catalyst support pellet. At least, the three parameter model should offer the same qualitative information regarding dispersal of impregnant as a function of particle radius as it does for axial position in the single pore. Quantitative information about the real system probably cannot be obtained from the single pore model (even if values of the parameters were known) because (1) a real network of pores would have a wide range of pore diameters and lengths, (2) fluid mixing in such a pore network is nonlinear, and (3) the geometry of a two-(cylindrical pellet) or three-(spherical) dimensional problem as opposed to a one-dimensional problem requires a different velocity $v_p(t)$ than was used in this work.

As an example of a three-dimensional solid which preserves the analytical simplicity of the single pore model consider a cylindrical pellet with a system of uniformly bifurcating pores extending from the center to the surface. The velocity as a function of time and the distance in from the surface can be shown to be:

$$v(z, t) = \frac{\Delta P R^2}{8 \mu S} 2^{(z-S)/S} \exp\left\{-\frac{\alpha \Delta P}{16 \mu}\left(\frac{R}{S}\right)^2 t\right\}, \tag{21}$$

where S is the length of the branches in the pore system and α is a constant approximately equal to 1.5 ln 2. In this geometry the velocity at any position in the pellet

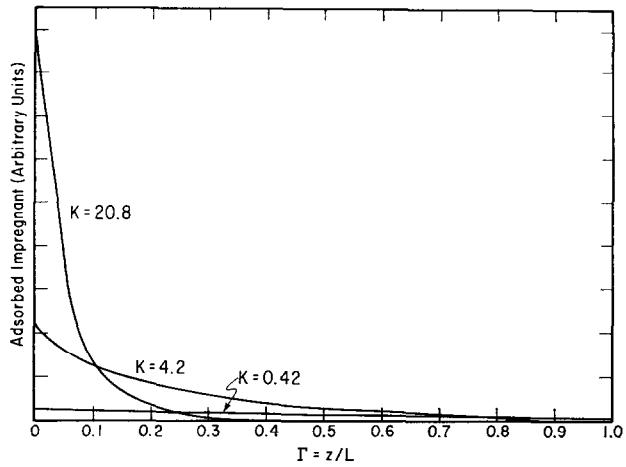

FIG. 5. Fractional coverage of pore wall vs axial position for nonsaturating, irreversible adsorption, case 2a; Eq. (20).

decreases exponentially with time rather than with the reciprocal of the square-root of time [Eq. (8)] as it does for the one-dimensional solid. Both results, however, are monotonically decreasing functions of time and though one might expect some quantitative differences, the qualitative features of the problem which this paper has tried to describe within the framework of the one-dimensional geometry should apply as well to three-dimensional systems. Further investigations of the single pore model for cylindrical and spherical geometries are planned in order to establish this point more definitely.

Empirical evidence of the qualitative validity of the model to real systems includes the work of Maatman (*3*) in which acid added to the impregnation solution evidently reduced η by occupying adsorption sites. Similar work done in this laboratory, and electron microprobe measurements of impregnant profiles in porous pellets by Andersen and Chen (*8*), also support the results presented here.

The upper photograph in Fig. 6 shows an alumina pellet which was soaked for 50 min in 0.5 M aqueous $NiCl_2$ (long enough for maximum water uptake), dried in air at 110°C and subsequently cut in half. The distinct dark band of nickel extending inward from the surface suggests that this is a system with a high value of K. The middle photograph shows a pellet treated similarly with an aqueous solution 0.5 M in $NiCl_2$ and 0.5 M in HNO_3. The light exterior band contains a low level of nickel (not evident in the photograph). This suggests that the acid sharply reduced the capacity of the support to adsorb nickel (reduced η) in this region, allowing the nickel to penetrate deeper into the pellet. When the acid was depleted (at the inner edge of the light band), the nickel adsorbed strongly in a subsurface band. The final photograph shows a pellet treated with 0.5 M $NiCl_2$ in concentrated HNO_3. Uniform impregnation was achieved since there was sufficient acid to reduce η throughout the pellet. Although not shown here, uniform impregnation also was obtained by soaking pellets in acid, drying, and then impregnating with 5 M $NiCl_2$ in water.

The results of Andersen and Chen (*8*) for impregnation of alumina pellets with chromic acid and chromium nitrate are shown schematically in Fig. 7. The chromic acid system (upper figure) is evidently one with a low value of K and/or K_L (weakly adsorbing). The profile is gently sloping, and as η is decreased by increasing c_0, the level of impregnation increases, much as Fig. 2 predicts for low K systems. The profiles for the chromium nitrate show the sigmoidal character of a high K system.

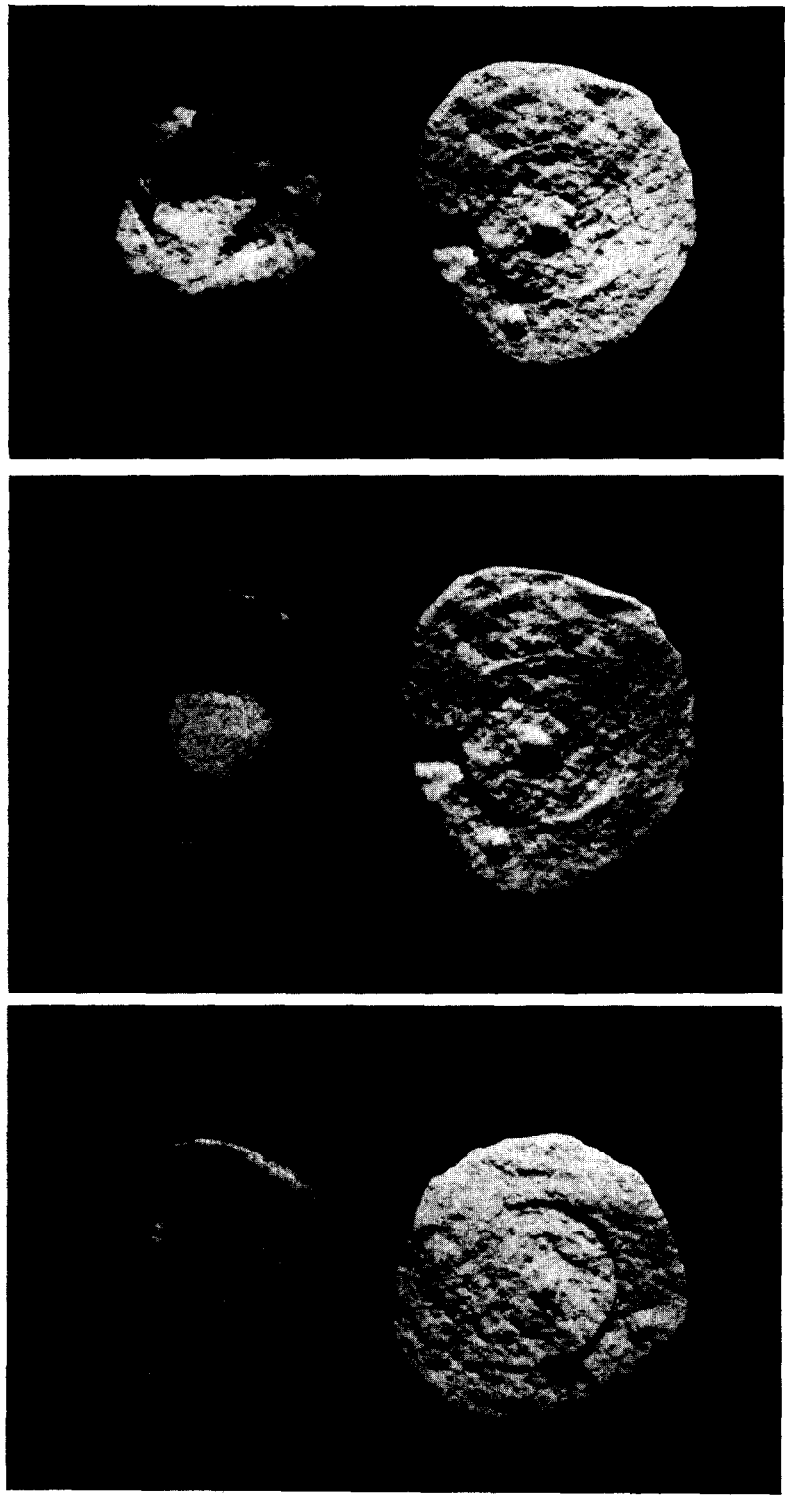

FIG. 6. Nickel impregnated alumina pellets. Upper: in 0.5 M $NiCl_2$ (aq); middle: in solution 0.5 M in $NiCl_2$ and 0.5 M in HCl; lower: in 0.5 M $NiCl_2$ in concentrated HCl.

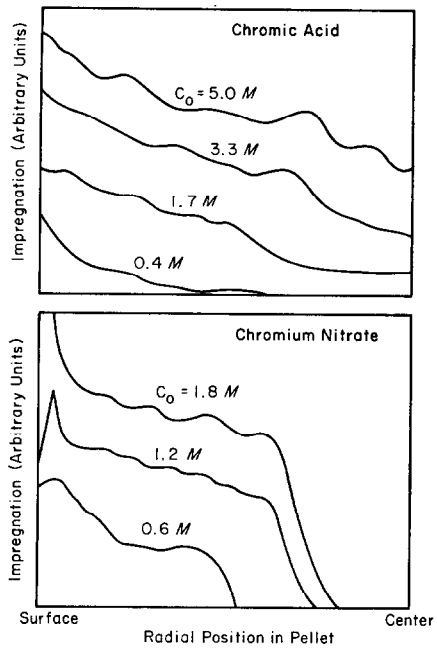

FIG. 7. Schematic reproduction of results of Andersen and Chen (*8*) with permission of the authors. Concentration of chromium vs radial position in alumina spheres.

The breakthrough advances as η is reduced, as in Fig. 3. The narrow region of very high metal content at the pellet surface is not predicted by the pore model. It may be due to a secondary process of crystallization or to precipitation during drying of the pellets.

The analytical solution of the irreversible adsorption kinetics (model 2a) represents an interesting limiting case when either the adsorptivity of the impregnant on the pore wall is very large or when the liquid concentration is very low. It would also be applicable to deposition by crystal growth and/or precipitation. In such cases and in ion-exchange impregnation the rate of attachment could be much smaller than the liquid phase mass transfer.

SUMMARY AND CONCLUSIONS

A single pore model has been developed to analyze the time-dependent problem of liquid phase impregnation of a catalyst pellet. The model employs the plug flow approximation, shown to be physically reasonable, with a liquid velocity proportional to $t^{-1/2}$. Two types of resistance at the solution–wall boundary, mass transfer and adsorption kinetics are shown to yield similar values of impregnation profiles in systems in which saturation occurs. The subcase of irreversible, kinetically controlled adsorption without saturation has been solved analytically. The results of the model qualitatively explain observations made on real three-dimensional systems.

Of the three independent parameters in the model, η is apparently the most useful in the management of impregnant dispersal. It is the most easily adjusted parameter and its effect has been demonstrated empirically. If the parameter K is large enough to yield the sigmoid impregnation profiles, adjustment of η should be a simple practical means of obtaining uniform impregnation to whatever depth desired.

APPENDIX

Solution to Eq. (11), Diffusion *in Plug Flow*

In order to avoid the problems of a simultaneous solution of a three-dimensional system with a discontinuous boundary condition, a direct numerical solution of Eq. (11) was not attempted. Rather, the following scheme was used.

The column of solution passing down the pore was divided mathematically into M cylindrical units or "slugs" which pass sequentially into and down the pore. Since the flow is plug and there is no desorption or axial diffusion, there is no mixing between slugs and a mass balance can be solved for each slug independently. The only restriction is that each slug be very short relative to the length in the "real" system over which appreciable axial concentration gradients would exist. The problem is solved by calculating how each slug disperses impregnant along the pore by diffusing it across the radial boundary and summing the contribution from all M slugs at each point along the pore. The discontinuous boundary condition at $r = R$ as θ changes from unity to less than unity is easily accommodated by this scheme.

The mass balance for each slug becomes

$$\frac{\partial c}{\partial t'} = \mathfrak{D}\,\frac{1}{r}\,\frac{\partial}{\partial r}\left(r\,\frac{\partial c}{\partial r}\right),$$

$$c(r, 0) = c_0, \quad c(R, t') = 0, \quad \left.\frac{\partial c}{\partial r}\right|_{r=0} = 0,$$

which is simply the well-known one-dimensional unsteady transport equation for a cylinder. Its solution for these boundary conditions is

$$c(r, t') = 2c_0 \sum_{n=1}^{\infty} \exp(-\mathfrak{D}\mathfrak{B}_n{}^2 t')\,\frac{J_0(\mathfrak{B}_n r)}{\mathfrak{B}_n J_1(\mathfrak{B}_n)},$$

$$\left.\frac{\partial c}{\partial r}\right|_{r=R} = 2c_0 \sum_{n=1}^{\infty} \exp(-\mathfrak{D}\mathfrak{B}_n{}^2 t'),$$

where J is the Bessell function, $J_0(\mathfrak{B}_n) = 0$, and t' measures time from when the slug first reaches a point in the pore for which $\theta < 1$.

The result of this scheme is that the adsorption at point z from the Nth slug is given by

$$I_N(Z) = 4c_0R^2 \sum \frac{1}{\mathfrak{B}_n{}^2} \exp(-\mathfrak{B}_n{}^2 \mathfrak{D}t') \Big|_{t'=t'_1}^{t'=t'_2},$$

where

$$t'_1 = \frac{t_L}{R^2}\,(z^2 - z_s{}^2)$$

$$t'_2 = \frac{t_L}{R^2}\left(\frac{R^2}{M} + z^2 - z_s{}^2\right)$$

and z_s is the smallest value of z for which $\theta < 1$.

A running summation $\Sigma_N I_N(z)$ is kept and compared with whatever saturation level is desired in order to adjust z_s as necessary. The final summation $\Sigma_{N=1}{}^{M} I_N(z)$ gives the impregnation profile.

References

1. Benesi, H. A., Curtis, R. M., and Studer, H. P., *J. Catal.* **10**, 328 (1968).
2. Schotten, J. J. F., and Van Montfoort, A., *J. Catal.* **1**, 85 (1962).
3. Maatman, R. W., *Ind. Eng. Chem.* **51**, 913 (1959).
4. Weisz, P., *Trans. Faraday Soc.* **63**, 1801 (1967).
5. Washburn, F. W., *Phys. Rev.* **17**, 273 (1921).
6. Levenspiel, O., *Chem. React. Eng.* 274 (1967).
7. Taylor, G. I., *Proc. Roy. Soc., Ser. A* **225**, 374 (1954a).
8. Chen, H. C., and Andersen, R. B., *Ind. Eng. Chem., Prod. Res. Develop.* **12**, 122 (1973).